

# Control of ion energy distribution at substrates during plasma processing

S.-B. Wang and A. E. Wendt<sup>a)</sup>

*Department of Electrical and Computer Engineering and Center for Plasma-Aided Manufacturing, University of Wisconsin—Madison, Madison, Wisconsin 53706*

(Received 15 December 1999; accepted for publication 23 February 2000)

Control of ion energy distribution functions (IEDF) at the substrate during plasma processing is achieved using a specially tailored voltage waveform for substrate bias, consisting of a short voltage spike in combination with a slow ramp. A much narrower IEDF is possible compared to the conventional approach of applying a sinusoidal waveform to the substrate electrode. Measurements in a helicon plasma combined with a time-dependent spherical-shell plasma fluid model demonstrate the benefits of this method in producing a narrow IEDF of precisely controllable energy, independent of ion mass. © 2000 American Institute of Physics. [S0021-8979(00)03411-3]

## I. INTRODUCTION

One of the primary advantages of plasma-assisted etching of materials over wet etching is directional etching due to energetic ion bombardment of the substrate. Plasma etching is indispensable in semiconductor manufacturing for reducing device size and increasing the aspect ratio of etched features. In typical manufacturing plasma processes, ion energy is coarsely controlled by varying the amplitude of a rf sinusoidal bias voltage applied to the substrate electrode, but the resulting ion energy distribution function (IEDF) is generally broad.<sup>1,2</sup> The energy provided to the substrate surface upon ion impact can enhance chemical reactions via several mechanisms, demonstrated in simulation and ion beam experiments, with significant implications for etched feature profiles and etch selectivity,<sup>3,4</sup> as well as film quality in plasma enhanced physical vapor deposition (PECVD) processes.<sup>5</sup> Control of the width of the IEDF at the substrate has the potential for significantly improving these aspects of plasma processes, and for improving understanding of the role ions play.

Use of the conventional sinusoidal substrate bias for IEDF control is limited by physical constraints. The ion mean free path in the sheath region, the ion sheath transit time, and the substrate bias voltage waveform, which determines the sheath voltage drop between the plasma and the substrate, are primary factors that determine the IEDF at the substrate. In high pressure and/or high substrate voltage conditions typically used in reactive ion etching, the mean free path of ions is comparable to or even shorter than the sheath thickness. In that case, the IEDF at the substrate is broadened due to the collisions in the sheath region, regardless of the bias voltage waveform. However, high density plasmas (HDPs) for semiconductor processing, characterized by high plasma density, low pressure and lower average substrate voltage, typically have collisionless sheaths at the substrate. The typical IEDF at the substrate of HDP process tools is a bimodal curve, coalescing into a single peak when the substrate bias frequency is sufficiently high compared to the ion

plasma frequency. The variation in ion energy arises from the temporal modulation of the sheath voltage; if the ion transit time across the sheath is short compared to the rf period, the bombarding energy of any given ion will correspond to the sheath voltage at the moment it reaches the sheath edge. For ion transit time long compared to the rf period, the ion energy more closely corresponds to the average sheath voltage. Although increasing bias frequency is one route that has been discussed as a method for narrowing the IEDF,<sup>1</sup> it suffers from two fatal limitations. First, the width of the IEDF is ion mass dependent,<sup>6</sup> and, even for high bias frequencies, tends to be wide for low mass ions often produced in processing plasmas. Second, at sufficiently high frequencies, the rf wavelength becomes comparable to the substrate dimensions, and bias voltage nonuniformities across the substrate surface develop, leading to unacceptable process nonuniformities.<sup>7</sup>

## II. SIMULATION

The method introduced here does not suffer from these limitations, and excellent IEDF control is possible. In place of a sinusoidal waveform, it employs a periodic bias voltage waveform applied to the substrate electrode consisting of a short voltage spike in combination with a longer slow voltage ramp. This waveform produces a constant sheath potential drop during the ramp period, which constitutes most of each cycle, resulting in a narrow IEDF. The short high voltage pulses are needed to prevent charge accumulation on the substrate surface. The potential on the surface of the substrate rises briefly, permitting collection of electrons to neutralize positive charge associated with ion bombardment. A one-dimensional spherical-shell fluid model is used to simulate the IEDF at the substrate as the bias waveform applied to the substrate is modified. Experimental measurements of substrate and plasma potential in a helicon argon plasma system shown in Fig. 1 show strong agreement with the fluid model.

To estimate the IEDF for tailored substrate electrode bias voltage waveforms, a one-dimensional, spherical-shell fluid model is solved numerically for the radial dependence of plasma parameters. The inner and outer electrodes are

<sup>a)</sup>Electronic mail: wendt@engr.wisc.edu

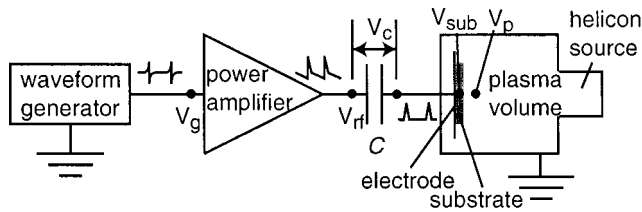


FIG. 1. Schematic diagram of system, showing major components, and voltages monitored in the simulation and experiment. The geometry of the plasma region corresponds to that of the experiment; in the simulation, the electrodes are concentric spherical shells.

treated as powered and grounded electrodes, respectively, with radii  $R_i$  and  $R_o$  selected to approximate the electrode area ratios typical of HDP process tools. A capacitor  $C$  is included in the model between the substrate and power supply to represent the combined capacitance of matching network components and insulating layers on the electrode and/or substrate, and is set to 0.161 nF for all cases simulated. The unmagnetized plasma fluid model is based on time-dependent hydrodynamic equations for the ions, described in detail in Ref. 8. Electrons are assumed to satisfy the Boltzmann relation, and the electron temperature  $kT_e$  is set at a constant value of 3 eV (typical for HDP etching plasmas) throughout this study. Starting with initial guesses, the ion density and velocity radial profiles are advanced in time by solving the momentum and continuity equations using the 4th order Runge Kutta method. With boundary conditions for the electric potential specified on the inner and outer electrodes (the outer electrode is always grounded, while the inner electrode is powered by applying a bias voltage waveform to the backside of capacitor  $C$ ), the radial potential profile in the plasma is obtained using the relaxation method to solve Poisson's equation at each time step. A variable grid spacing is used so that finer and coarser meshes can be applied to the sheath and bulk plasma regions, respectively. The plasma loss rate to the wall is held fixed at a value corresponding to a Bohm flux for an ion density  $10^{11} \text{ cm}^{-3}$  at the sheath edge, resulting in bulk plasma densities of  $10^{11} - 10^{12} \text{ cm}^{-3}$ , the typical range for HDP plasmas. The potential on the surface of the substrate is computed by considering the applied bias voltage waveform, the surface charge density on the substrate surface, and the space charge density in the sheath region.

Both space and time are discretized in the simulation. Because the accuracy of the calculated IEDF and ion energy at the substrate directly depend on the accuracy of the plasma parameters in the sheath region, 493 grid points divide the one-dimensional space of length  $L = R_o - R_i = 400\lambda_D$ , where  $\lambda_D$  is the Debye length. The mesh spacing varies from  $\lambda_D/16$  at the electrodes to  $4\lambda_D$  in the center of the plasma. The radius of the inner electrode is set as  $R_i = 200\lambda_D$  so that the area ratio of the outer electrode (grounded) to the inner electrode (powered) is 9. To simulate typical HDP operating conditions, we examine a 20 mTorr argon plasma.

Figure 2 shows an applied rf voltage,  $V_{rf}$ , that produces a narrow IEDF, as well as the associated waveforms for the voltage across the capacitor,  $V_C$ , the substrate potential,

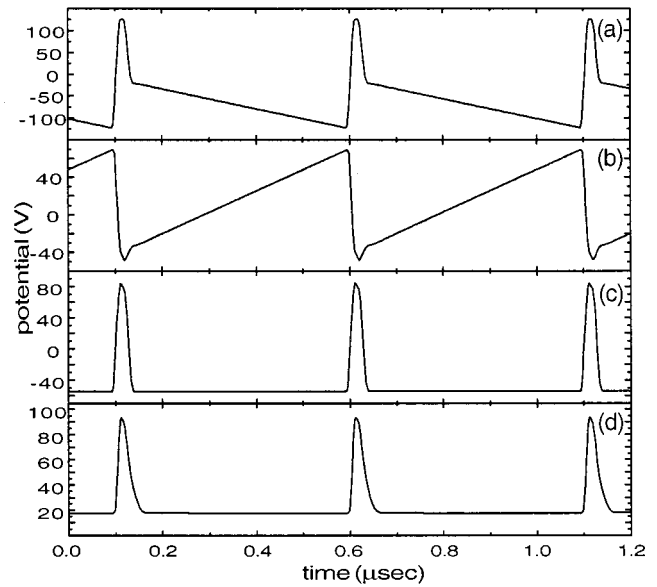


FIG. 2. Simulated voltage waveforms: (a) Assumed power supply output,  $V_{rf}$  (b) voltage across coupling capacitor,  $V_C$ , (c) substrate potential,  $V_{sub}$ , and (d) plasma potential,  $V_p$ .

$V_{sub}$ , and the plasma potential,  $V_p$  (see Fig. 1). The repeated applied rf voltage waveform,  $V_{rf}$ , consists of a high voltage pulse of width  $0.035 \mu\text{s}$ , followed by a slow, linear voltage ramp, with a repetition frequency of 2 MHz. The voltage ramp in the applied waveform  $V_{rf}$  is necessary to sustain a constant voltage  $V_{sub}$  on the substrate surface. The slope of the linear voltage decrease in time is chosen to compensate for the linear voltage increase across the capacitor  $V_C$  caused by the charge buildup on the substrate surface due to ion flux from the plasma. Without the ramp the sheath voltage, the difference  $V_p - V_{sub}$  between the plasma and substrate potentials, would vary linearly in time, resulting in a broad ion energy distribution.

Time-averaged IEDFs for argon ions are shown in Fig. 3, corresponding to three different bias voltage waveforms: Sinusoidal, pulsed with constant voltage between pulses, and pulsed with linear voltage ramp between pulses. The sinusoidal bias waveform is 160 V peak-to-peak, at a frequency

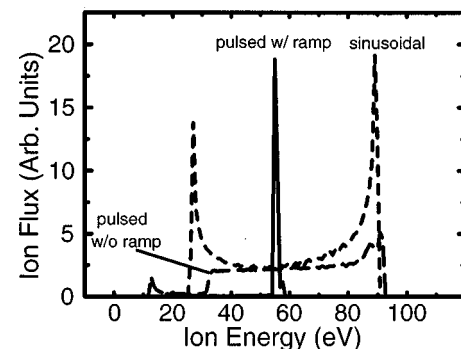


FIG. 3. The tailored bias voltage waveform consisting of periodic voltage spikes combined with a linear voltage ramp produces a narrow IEDF in simulation. For comparison, IEDFs are shown for the traditional sinusoidal waveform, and a pulsed waveform with constant voltage between spikes.

of 13.56 MHz, and produces the familiar bimodal IEDF. For the pulsed cases, the height of the voltage spikes is chosen to be approximately 200 V, in order to produce an average ion energy at the substrate similar to that in the sinusoidal case, about 58 eV. The case with the voltage ramp between pulses produces a much narrower IEDF than the other two cases because the sheath voltage remains constant between pulses. The sheath transit time for the ions is short compared to the pulse period, so the energy of each ion depends on the instantaneous potential drop when it enters the sheath. Although the result shown is for argon ions only, we expect the same result ions of all masses, because the period between pulses, over which the sheath voltage is constant, is small compared to the sheath transit time for even the lightest ions.

### III. EXPERIMENT

All experiments were carried out in a helicon plasma etch tool built in house. The cylindrical chamber is made of stainless steel with inner diameter 50 cm and height 75 cm. As in the simulation, the grounded wall area is much greater than the area of the 10 cm diameter substrate electrode. The helicon antenna supplies 1000 W at 13.56 MHz to sustain the 20 mTorr argon plasma. The tailored bias voltage is applied to the substrate electrode by a broad band power amplifier (ENI A500) driven by a programmable arbitrary waveform generator. The power amplifier is connected to the substrate electrode through a capacitor of capacitance 3.42 nF. The substrate potential is measured with a Langmuir probe stuck on the surface of the silicon substrate while the plasma potential is monitored with an emissive probe.<sup>9</sup> In this experimental setup, no matching network is employed between the power amplifier and substrate electrode, in contrast to typical configurations for the conventional sinusoidal bias. The tailored waveform consists of many frequency components, while conventional matching networks are tuned for a single frequency and are therefore unsuitable for this application.

Results with a pulse waveform with pulse width 0.2  $\mu$ s, pulse period of approximately 2  $\mu$ s, and compensating slope are shown in Fig. 4. The shape of the waveform generator output [Fig. 4(a)],  $V_g$ , is tailored to compensate for the frequency dependence of the power amplifier gain, so that the amplifier output [Fig. 4(b)],  $V_{rf}$ , has the desired form. The voltage on the electrode side of the capacitor [Fig. 4(c)] shows a constant voltage between the spikes, as does the voltage on the surface of the silicon substrate [Fig. 4(d)],  $V_{sub}$ . The impedance mismatch between the cable to the substrate electrode and the load results in power reflection, and hence, an ‘‘echo’’ pulse may be observed in the measured waveforms immediately after the applied voltage spike. The 50  $\Omega$  impedance at the power amplifier output matches that of the cable, preventing further reflections.

A straight slope between pulses can be seen in the power amplifier output,  $V_{rf}$ , shown in Fig. 4(b). As predicted by the simulation, the straight line results from the ion current to the surface of the substrate. From this slope, the ion bombarding flux can be noninvasively computed using the voltage waveform, serving as a monitor for drifts in plasma conditions. The average value (‘‘self-bias’’) of the substrate potential,

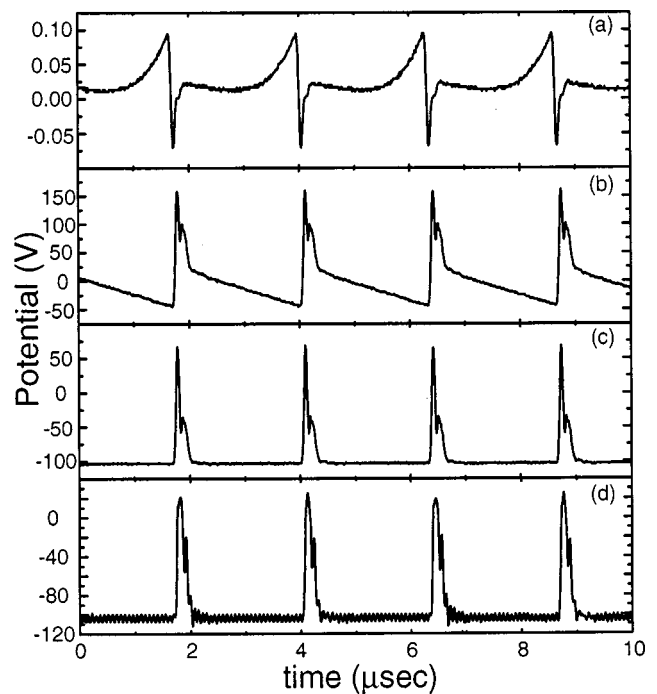


FIG. 4. Measured voltages: (a) waveform generator output,  $V_g$  (b) power amplifier output,  $V_{rf}$  (c) electrode voltage, and (d) voltage on surface of silicon substrate,  $V_{sub}$ .

$V_{sub}$ , between spikes [Fig. 4(d)] matches that measured at the electrode from outside the vacuum chamber as shown in Fig. 4(c). Thus, the dc self-bias voltage, which determines the energy of the bombarding ions, can be monitored externally, avoiding the impractical approach of attaching a probe to the front surface of the substrate.

Figure 5 shows simultaneous measurements of the plasma potential,  $V_p$ , and substrate potential,  $V_{sub}$ . As in the simulation,  $V_p$  shows short transients corresponding to the substrate potential spikes, quickly recovering to the steady state value. The difference between  $V_p$  and  $V_{sub}$  is the voltage drop across the plasma sheath in front of the substrate, and is nearly constant (aside from noise) between spikes. Electrons from the plasma are collected by the substrate only in the short high-voltage spike periods, when the sheath volt-

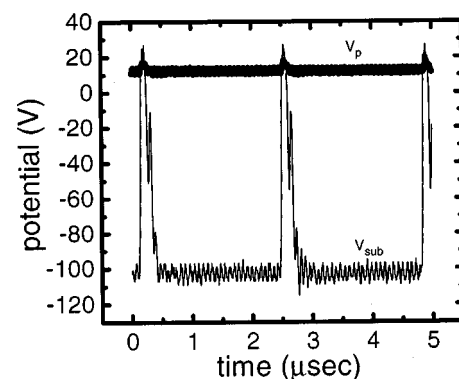


FIG. 5. The difference between the plasma potential,  $V_p$  and the substrate potential,  $V_{sub}$ , is the sheath potential, which determines the energy of ions reaching the substrate.

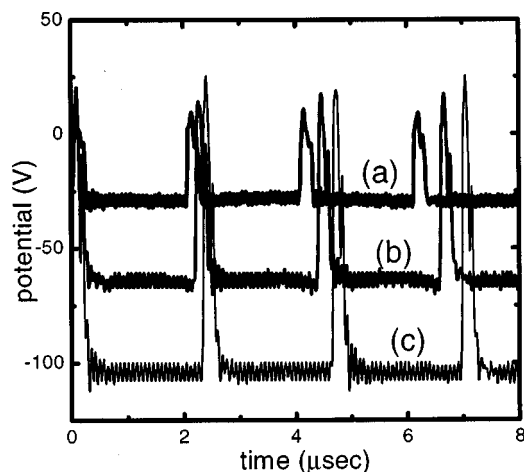


FIG. 6. Different values of dc self-bias voltage on the substrate [(a)–(c)] can be achieved using the same waveform shape stored in the waveform generator. Increasing the amplitude of the generator output results in a larger magnitude of the self-bias voltage, but then the repetition frequency must also be decreased to maintain the desired compensating slope between spikes.

age drops low enough that they can overcome the electrostatic potential barrier. Most ions are collected in the off-spike period, and, since ion energy at the substrate is determined by the sheath potential drop, we believe that the nearly constant sheath voltage during that period is a strong indication of a narrow IEDF, as found in the simulation (Fig. 2). A direct measurement of the IEDF is more challenging<sup>10</sup> than the sheath voltage measurement performed here, and is planned as a future experiment.

In order to control the energy of the ions bombarding the substrate the value of the dc self-bias voltage must be adjusted. To increase the dc self-bias voltage the height of the spikes in the applied waveform must be increased. In the experimental measurements of substrate potential shown in Fig. 6, this was achieved by increasing the amplitude of the waveform generator output shown in Fig. 4(a), without altering its basic shape. However, the repetition frequency must simultaneously be adjusted to preserve the slope of the linear

voltage ramp between spikes. That slope is determined by plasma conditions; it must be set to exactly compensate for positive charge accumulation on the surface of the substrate due to ion flux, in order to maintain a constant substrate voltage between spikes.

#### IV. CONCLUSIONS

The application of this method for IEDF control has implications for better understanding ion–surface interactions during plasma processing, as well as potential for improving control over process outcome. While previous efforts to examine the role of ion bombardment energy in plasma processing have succeeded in a controlled environment,<sup>5</sup> this technique opens the possibility of studying the role of ion energy *in situ* under realistic process conditions. With a narrow IEDF in etching processes, selectivity may be improved by positioning the ion energy between the threshold energies of two materials. The IEDF also plays a role in feature profile evolution,<sup>3</sup> and its control may both improve understanding of the factors involved and provide a means to better control the resulting profile. Finally, research in PECVD processes has shown the importance of ion energy in controlling the quality of deposited films,<sup>5,11</sup> even with the relatively broad IEDFs obtained with a sinusoidal bias. Improved control of film quality can be expected with the more precisely controlled IEDF obtained with this technique.

<sup>1</sup>W. M. Holber and J. Forster, J. Vac. Sci. Technol. A **8**, 3720 (1990).

<sup>2</sup>J. Hopwood, Appl. Phys. Lett. **62**, 940 (1993).

<sup>3</sup>G. S. Hwang and K. P. Giapis, J. Vac. Sci. Technol. B **15**, 70 (1997).

<sup>4</sup>E. Collard, C. Lejuene, J. Grandchamp, J. P. Gilles, and P. Scheiblin, Thin Solid Films **193**, 100 (1990).

<sup>5</sup>L. Martinu, J. E. Klemberg-Sapieha, O. M. Kuttel, A. Raveh, and M. R. Wertheimer, J. Vac. Sci. Technol. A **12**, 1360 (1994).

<sup>6</sup>A. D. Huypers and H. J. Hopman, J. Appl. Phys. **67**, 1229 (1990).

<sup>7</sup>J. E. Stevens, M. J. Sowa, and J. L. Cecchi, J. Vac. Sci. Technol. A **14**, 139 (1996).

<sup>8</sup>S.-B. Wang and A. E. Wendt, IEEE Trans. Plasma Sci. **27**, 1358 (1999).

<sup>9</sup>N. Hershkovitz, B. Nelson, J. Pew, and D. Gates, Rev. Sci. Instrum. **54**, 29 (1983).

<sup>10</sup>J. Liu, G. L. Huppert, and H. H. Sawin, J. Appl. Phys. **68**, 3916 (1990).

<sup>11</sup>K. L. Seaward, J. E. Turner, K. Nauka, and A. M. E. Nel, J. Vac. Sci. Technol. B **13**, 118 (1995).